# Application of Model-Matching Techniques to Feedforward Active Noise Controller Design

Jwu-Sheng Hu, Shiang-Hwua Yu, and Cheng-Shiang Hsieh

***Abstract*— In this paper, three digital model-matching techniques in $H_2$, $H_\infty$, and $l_1$ performance measures are applied to design digital feedforward controllers for active noise cancellation in ducts. Different measures account for different optimization objectives in terms of physical signals. The distributed nature and high-bandwidth requirements of the control system result in a large set of parameters in plant description and these design techniques proved to be useful in solving the controllers numerically. Experiments were conducted using a floating-point digital signal processor that produced broad-band noise reduction. Design variations and noise reduction effects in terms of human perception are also discussed. It is experimentally proved that using model-matching designs, the causality principle originally raised by Paul Lueg does not have to be satisfied in order to actively reduce the noise level.**

***Index Terms*—Acoustic noise, active noise cancellation, digital filters, digital signal processors, H-*infinity* optimization, model matching methods.**

## I. Introduction

MODEL-MATCHING techniques are fundamental to a wide variety of linear control systems design problems [6], [17], [33]. While many feedback control problems can ultimately be formulated as model-matching problems, the most straightforward application is to design feedforward controllers [11], [18], [28]–[30], [35]. Generally speaking, a feedforward controller has to invert the plant in a certain way, i.e., making the signal path from reference input to output as close to identity as possible. To characterize the word "close," several mathematical indexes such as the $\mathbf{H}_\infty$-norm (maximum amplitude of a transfer function) or $\mathbf{H}_2$-norm (energy of the impulse response) fit naturally into the picture. As a result, model-matching techniques based on these measures have become very useful in designing feedforward controllers [31].

Basically, optimization of various error measures is the key to these techniques. However, there are two different approaches to deal with the design problem. When reference or disturbance signal types are known, e.g., step or sinusoidal functions, it is necessary to include the signal in the error measure. Usually this is accomplished by directly optimizing the error signal in different time-domain measures [15]. For unknown signal types (e.g., random or nonstationary), the optimal solutions are obtained by considering worst case scenarios. Consequently, instead of minimizing error signals, deviation of signal paths from identity is optimized.

This paper describes the application of model-matching techniques to designing digital feedforward active noise controllers. As an effective way of reducing low-frequency noise, active noise control methods have drawn much attention in recent years [12], [23]. Perhaps the most popular controller-design approach is based on the least mean square (LMS) algorithm originally developed by Widrow [36]. Although many modifications of this algorithm have been developed [7], [8], the basic controller structure applied to active noise cancellation is as shown in Fig. 1.

The dotted line in Fig. 1 represents the controller's tuning path. Several modifications are done when $d(k)$'s measurement contains the influence of acoustic feedback from the control speaker. From this figure, it is quite clear that for persistently-excited noise inputs, LMS actually tries to solve the model-matching problem on-line with respect to the least-mean-square measure. The ideal controller $C$ (a perfect match) must fulfill

$$E(z^{-1}) = T_1(z^{-1}) - T_2(z^{-1})C(z^{-1}) = 0 \tag{1}$$

or

$$C(z^{-1}) = T_2^{-1}(z^{-1})T_1(z^{-1}). \tag{2}$$

In most cases (2) cannot be satisfied due to nonminimum phase zeros and delay steps (which correspond to zeros at infinity). Attempts have been made to approximate the inverse by curve-fitting the spectrum of $C(z^{-1})$ using an FIR filter [27]. In that case, only the $T_1$ and $T_2$ spectra are required.

From the discussion in the preceding paragraph, it is clear that selecting $C(z^{-1})$ (Fig. 1) off-line can be cast as a model-matching problem. Further, from the design standpoint, this is almost identical to a tracking design problem. Recent progress in tracking control shows the value of using preview steps in designing feedforward controllers [1], [13], [22], [25], [31], [32]. Preview steps are necessary to minimize the effect of nonminimum phase zeros which are common in sample-data systems when both sampling rates and relative degrees are high [2]. In order to use preview steps, future information on reference or disturbance signals is required. For active noise control systems, the hardware configuration is usually arranged such that the noise transmission path is longer than the control sound transmission path (see Fig. 1). In other words, $T_1$ has more delay steps than $T_2$ in the sense that a signal is injected simultaneously into both paths. The difference in delay steps

Manuscript received March 19, 1996; revised June 2, 1997. Recommended by Asociate Editor, E. G. Collins, Jr. This work was supported by the National Science Council of Taiwan under Grant NSC84-2732-E009-009.

The authors are with the Department of Control Engineering, National Chao-Tung University, Hsinchu, Taiwan, R.O.C.

Publisher Item Identifier S 1063-6536(98)00578-8.

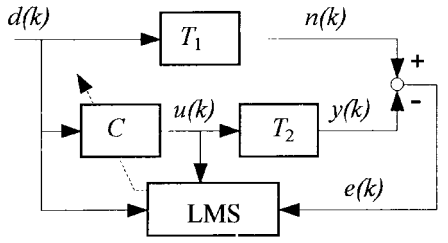


$T_1$ transfer function of the noise transmission path
$T_2$ transfer function of the control sound transmission path
$C$ controller
$d(k)$ noise source signal
$e(k)$ error microphone signal
$u(k)$ control input

Fig. 1. The controller structure using LMS algorithms.

is therefore equivalent to preview steps when formulated as a tracking problem. Other than the effect of nonminimum phase zeros, preview steps are also required to satisfy the causality principle first raised by Lueg [20]:

> "An acoustic wave with a specific frequency has a relatively much lower speed than an electrical signal of the same frequency. This implies that, while a sound wave is traveling from a point where it is detected to a point where it is to be attenuated, there is enough time available within the electronic circuit to process the signal and activate the control elements, to a greater or lesser degree, depending on the frequency, type of noise, and physical extent of the system."

While the description provides a clear explanation of an active noise cancellation mechanism, an interesting question arises: can noise levels be actively reduced when the causality principle is violated? As explained and experimentally proved later, through model-matching techniques, the answer is "yes."

Three model-matching techniques in the digital single input/single output (SISO) domain are applied in this paper ($\mathbf{H}_2$, $\mathbf{H}_\infty$, and $\mathbf{l}_1$ norm). All these techniques assume that the type of noise is unknown (i.e., worst case optimization). A common application of the theory is to design the controller in the continuous-time domain and implement it using high-speed digital processors. But for some complicated high-bandwidth systems, the limited computation power of microprocessors may result in less than truly continuous-time control laws. Therefore, it is vital in these cases to begin with digital design techniques [4]–[6], [10], [33]. The formulation and design procedure shown in Sections II and III of this paper are essentially the same as in [31] where a more complete treatment of the theory could be found.

Experiments were conducted on a rectangular duct, and control algorithms were implemented on a TMS320c30 based DSP system. In addition to objective evaluations of various design approaches (e.g., noise spectrum dB reduction), subjective evaluations were also conducted by measurement with a weighted sound level meter (e.g., A-weighting). Like most feedforward-types of LMS algorithms, the model-matching approach requires to measure the noise signal with a minimum effect of acoustic feedback. Since the controller is designed off-line, it cannot accommodate possible changes of the dynamics ($T_1$ and $T_2$ in Fig. 1). However, it offers the optimal solution and does not have any parameter convergence problems. As a result, the method can be used as a bench mark to check the performance of an adaptive algorithm in broad-band noise reduction. Second, the simple controllers architecture (a single filter and no error microphone) can be used in some cases where the cost is of primary concern.

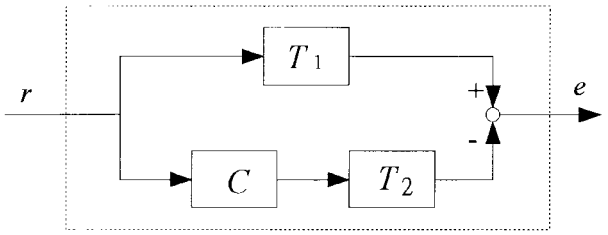


$H = T_1 - T_2 C$ ( a linear time invariant system)

Fig. 2. Model-matching block diagram.

TABLE I

| | |
|---|---|
| $\mathbf{H_2}$ norm | $\|T_1 - T_2C\|_2 = \sup\{\|e\|_\infty : \|r\|_2 \le 1\}$ |
| $\mathbf{H}_\infty$ norm | $\|T_1 - T_2C\|_\infty = \sup\{\|e\|_2 : \|r\|_2 \le 1\}$ |
| $\boldsymbol{l_1}$ norm | $\|T_1 - T_2C\|_{A_d} = \sup\{\|e\|_\infty : \|r\|_\infty \le 1\}$ |

## II. Model-Matching Problems

Model-matching problems can be stated as follows.

Given linear time-invariant, proper, stable systems $T_1$ and $T_2$ (see Fig. 2), design a proper stable controller $C$ such that the response to exogenous inputs is minimized; that is

$$\underset{C \in \mathbf{RH}_\infty}{\text{Min}} \|T_1 - T_2 C\| \tag{3}$$

where $\mathbf{RH}_\infty$ denotes the set of proper, stable, and real-rational transfer functions.

The configuration shown in Fig. 2 is sometimes called the one-block problem. We might get different optimal solutions according to different cost measures (e.g., $\mathbf{H}_2$, $\mathbf{H}_\infty$, and $\mathbf{l}_1$ norm). For more explanations of these norms, please refer to [6], [10], [31], and [35]. These measures are concerned with the least upper bound of the output response subject to a certain group of input signals (see Table I). For example, when inputs are modeled as bounded-energy signals and the response is measured in terms of energy, this leads to an $\mathbf{H}_\infty$ model-matching problem.

TABLE II
OPTIMAL MODEL MATCHING SOLUTIONS TO $T_2(z^{-1}) = G(z^{-1})(1 - az^{-1})$ WHERE $G(z^{-1})$ IS A UNIT IN $\mathbf{RH}_\infty$ AND $\infty > |a| > 1$

| | Optimal $C$ | Error function $1 - T_2C$ | Error norm |
|---|---|---|---|
| $\mathbf{H_2}$ | $\dfrac{\left(\frac{1}{a^2}-1\right)\left[\left(\frac{z}{a}\right)^N + \left(\frac{z}{a}\right)^{N-1} + \cdots + \left(\frac{z}{a}\right) + \frac{1}{1-a^2}\right]}{1 - \frac{1}{a}z^{-1}} G^{-1}(z^{-1})$ | $\left(\dfrac{1-a^2}{a^{N+1}}\right)\dfrac{z^N}{1-az^{-1}}$ | $\dfrac{\sqrt{a^2-1}}{\lvert a^{N+1}\rvert}$ |
| $\mathbf{H}\infty$, $l_1$ | $-\left(\frac{1}{a^N}z^N + \frac{1}{a^{N-1}}z^{N-1} + \cdots + \frac{1}{a}z\right)G^{-1}(z^{-1})$ | $\dfrac{1}{a^N}z^N$ | $\left\lvert\dfrac{1}{a^N}\right\rvert$ |

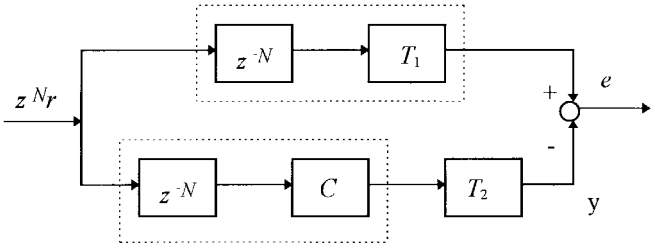


Fig. 3. The structure of a preview model-matching problem ($N$: number of preview steps).

If $T_2$ is minimum phase and its relative degree is zero (i.e., no zeros at infinity), the optimal solution is trivial ($C = T_2^{-l}T_1$) and the infimal cost is zero. In the remaining discussion, it is assumed that $T_2$ is nonminimum phase and it has no zeros on the unit circle. Solutions to (3) for the three commonly used norms can be found in [31].

If the future signal of $r$ (Fig. 2) is available, it is desirable to allow the controller be noncausal (or nonproper) to obtain a better response. This leads to the so-called preview model-matching problem (also see [31]). Denoting $z$ as the $z$-transform variable, the equivalent block diagram can be shown as Fig. 3 where the constraint on the controller now becomes $z^{-N}C \in \mathbf{RH}_\infty$.

Further, depending on applications, performance on a particular frequency range might need to be emphasized. This is usually achieved by incorporating a weighting function in (3). As a result, the optimization problem is written as

$$\underset{z^{-N}C \in \mathbf{RH}_\infty}{\text{Min}} \|z^{-N}W(T_1 - T_2C)\| \tag{4}$$

where $W$ denotes a weighting function.

Consider a simple example in which the plant $T_2$ has only one real unstable zero at $a$ and no zeros on the unit circle; that is

$$T_2(z^{-1}) = G(z^{-1})(1 - az^{-1})$$

where

$$G(z^{-1}) \text{ is a unit in } \mathbf{RH}_\infty \text{ and } \infty > |a| > 1.$$

Let $T_1 = 1$ and weighting function $W = 1$. With $N$ preview steps, the optimal $C$'s can be solved for and corresponding minimum error norms that result are shown in Table II.

It is not surprising that the $\mathbf{H}_\infty$ and $\mathbf{l}_1$ optimizations in this case are the same (see [1] and [35]); but the results reveal an interesting phenomenon, e.g., the presence of a truncated Laurent series of $B^{-1}(z^{-1})$ at every point inside the region of convergence, i.e.,

$$\frac{1}{1 - az^{-1}} = -\frac{1}{a}z - \frac{1}{a^2}z^2 - \frac{1}{a^3}z^3 \cdots \qquad |z| < a. \tag{5}$$

If we define $[\bullet]_N$ as the truncation of Laurent series to the $N$th order term, the $\mathbf{H}_\infty$ and $\mathbf{l}_1$ optimizations in this case are simply $[B^{-1}(z^{-1})]_N G^{-1}(z^{-1})$. Furthermore, Table II shows that the $\mathbf{H}_2$ optimization also contains the truncated series as

$$C(z^{-1})\Big|_{\mathbf{H}_2\text{optimal}} = \frac{1}{\overline{B}(z^{-1})}\left[\frac{\overline{B}(z^{-1})}{B(z^{-1})}\right]_N G^{-1}(z^{-1}). \tag{6}$$

Equation (6) is also a general solution where $\overline{B}(z^{-1}) = B(z)z^{-m}$ and $m$ is the number of unstable zeros. The following remarks list some further observations.

*Remark 2.1:* All solutions in Table II converge to $B^{-1}(z^{-1})$ as $N$ approaches infinity. That is to say, when $N$ is large, the difference among solutions may not be significant.

*Remark 2.2:* The error norms in Table II decrease drastically as $N$ increases if $|a| \gg 1$. However, the coefficients of higher order terms in the truncated series become too small to have significant influence on performance in practical applications. This agrees with the experimental results presented by Alter and Tsao [1] which show that increasing $N$ provides no benefit after a certain preview length. Moreover, when $|a| \approx 1$, the improvement is not significant unless a very large $N$ is selected.

*Remark 2.3:* When the preview length is zero, it can be seen from Table II that zero is the solution to both $\mathbf{H}_\infty$ and $\mathbf{l}_1$ optimizations. In fact, this solution applies to general cases (more than one unstable zero). In $\mathbf{H}_\infty$, the reason is quite simple since the Pick matrix reduces to zero [33]. Since the error norm in $\mathbf{l}_1$ is no smaller than the corresponding norm in $\mathbf{H}_\infty$, its optimal value is one also. Through simple deduction, the optimal controller is identical to zero.

*Remark 2.4:* The message given by the analysis in Remark 2.3, is that one has to resort to suboptimal designs in $\mathbf{H}_\infty$ and $\mathbf{l}_1$ when equal performance measures in all frequency bands are desired [$W = T_1 = 1$ in (4)] and no preview step is allowed. But this is not true in the $\mathbf{H}_2$ context where a causal

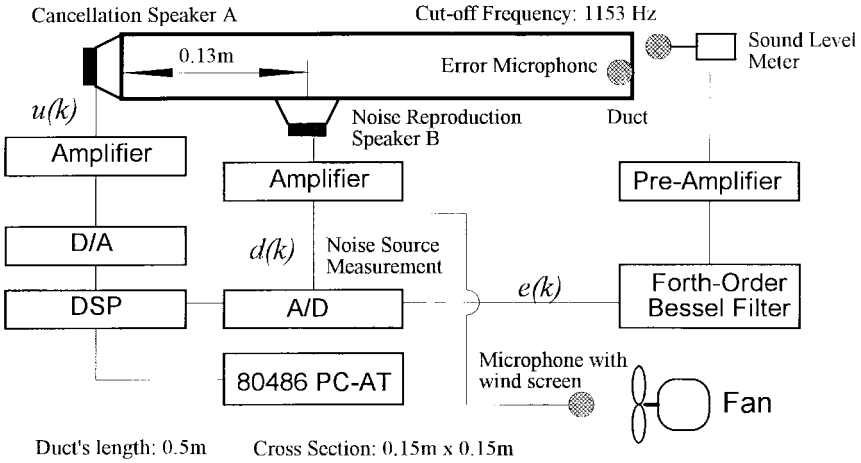


Fig. 4. Configuration of the experimental setup.

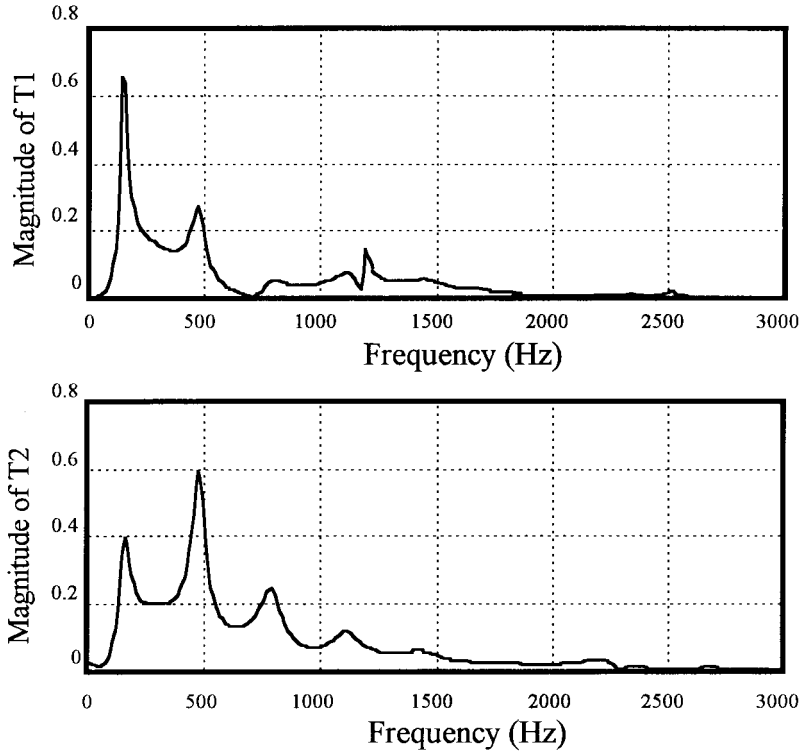


Fig. 5. Frequency response of the transfer functions $T_1$ and $T_2$.

solution is [see (6)]

$$C(z^{-1})\Big|_{\mathbf{H}_2\text{optimal, no preview}} = \frac{b_0/b_m}{\overline{B}(z^{-1})}\, G^{-1}(z^{-1}) \quad (7)$$

where

$$B(z^{-1}) = b_0 + b_1 z^{-1} + \cdots + b_m z^{-m}.$$

## III. Experimental Setup

Referred to Fig. 4, the experiments were conducted using a rectangular duct made of plastic glass. One end of the duct was left open and a control speaker (speaker A) was mounted on the other end to generate the cancellation signal. Another speaker (speaker B) was mounted on the side of the duct to simulate noise source. It was assumed that the signal [$d(k)$ in Fig. 4] driving speaker B was available and could be previewed. An error microphone and a sound level meter were placed at the open end of the duct to measure the error signal and the weighted average decibel reduction. The measurement of the error signal was filtered by a fourth-order Bessel filter with a cutoff frequency around 1 kHz. This frequency was arbitrarily selected but below the cutoff frequency of the duct (about 1153 Hz). Readers without extensive acoustic background may refer to the book by Pierce [24] for a better understanding of the term "duct's cutoff frequency." The feedforward control law was implemented by a TMS320C30-based DSP system equipped with 16-bit AD/DA channels. The DSP system was hosted by a 486-based PC-AT that stored data

TABLE III
POLES AND ZEROS OF TRANSFER FUNCTIONS $T_1$ AND $T_2$

| $T_1$ | | $T_2$ | |
|---|---|---|---|
| zeros | poles | zeros | poles |
| -2.2160 | -0.8623 ± 0.4719i | -6.8843 | 0.9669 ± 0.1522i |
| -0.9731 ± 0.4477i | -0.9146 ± 0.1272i | -1.4927 | 0.9441 |
| -0.7714 ± 0.7197i | -0.8858 ± 0.2779i | -0.8743 ± 0.5919i | 0.8573 ± 0.4603i |
| -0.9566 ± 0.2475i | -0.7333 ± 0.6524i | -0.8640 ± 0.1917i | 0.8533 ± 0.2620i |
| -0.8577 | -0.6203 ± 0.6950i | -0.7122 ± 0.6765i | 0.6483 ± 0.7010i |
| -0.4727 ± 0.9819i | -0.3201 ± 0.8822i | -0.2936 ± 0.8096i | 0.6486 ± 0.6029i |
| 1.0078 ± 0.0274i | -0.1328 ± 0.9358i | -0.0053 ± 0.8336i | 0.3768 ± 0.8656i |
| 0.7400 ± 0.6634i | 0.0491 ± 0.9212i | 0.3070 ± 0.8263i | 0.2679 ± 0.8249i |
| 0.7953 ± 0.3723i | 0.3181 ± 0.9365i | 0.6078 ± 0.6072i | 0.0568 ± 0.9104i |
| 0.3374 ± 0.9355i | 0.3608 ± 0.8650i | 1.0236 ± 0.0523i | -0.0802 ± 0.7971i |
| -0.1049 ± 0.8791i | 0.6583 ± 0.6996i | 0.6308 ± 0.3183i | -0.9202 ± 0.1253i |
| 0.4180 ± 0.4887i | 0.8568 ± 0.4588i | 0.6296 | -0.8742 ± 0.3042i |
| -0.1152 ± 0.6493i | 0.9774 ± 0.1500i | 0.2054 ± 0.4479i | -0.2849 ± 0.8461i |
| | 0.8295 ± 0.2151i | | -0.7728 ± 0.5563i |
| | 0.7651 ± 0.3299i | | -0.6902 ± 0.6794i |
| | 0.0367 ± 0.5122i | | -0.5694 ± 0.6492i |
| | -0.0557 | | -0.3064 ± 0.5618i |
| Delay = 11, Gain = 0.0057 | | Delay = 13, Gain = 0.0043 | |

and provided a man-machine interface. Sampling rate of the control system was set at 6 kHz.

The meaning of signals $d(k)$, $u(k)$, and $e(k)$ are identical to those used in Fig. 1. Furthermore, the transfer functions $T_1$ and $T_2$ also comprised of dynamic models of various electronic components and the duct. The noise signal $d(k)$ was generated by measuring the fan noise and broadcasted through speaker B. Notice that by simultaneously exciting both speakers, the sound produced by speaker A lagged behind the sound from speaker B by about 0.36 ms (at 25°C, the speed of sound in air is about 346 m/s) which corresponds to about 2.2 samples in the digital domain. This was deliberately arranged to obtain results that violated the causality principle.

The plants $T_1$ and $T_2$ were identified by injecting pseudo-random signals into both speakers and measuring output responses at error microphone. The time-domain least square algorithm was applied to obtain their coefficients. Table III shows the results in pole/zero form.

The frequency responses (Fig. 5) show the various resonant frequencies of the duct. If plane-wave approximation is considered, the boundary conditions of the duct can be assumed to be pressure-released (at the open end, see [24, p. 350]) and hard-walled (at speaker A). Its resonant frequencies are (see [16])

$$\omega_n = \frac{(2n-1)\pi c}{2L}, \qquad n = 1, 2, \cdots$$

$c$: speed of sound, $L$: duct length

or

$$\omega_n = 173\,519\,865\cdots \text{ Hz}.$$

These frequencies do not match very well with the identification (see Fig. 5). One of the reasons is due to an inaccurate description of the boundary conditions. For example, as the driving frequency is increased, more energy leaks out of the open end and the pressure-released condition is no longer true. Second, since the duct length is rather short, the nonuniform pressure distribution (on the cross-section) induced by both ends may still have strong effect on the measurement. Hence, the physical mechanism of sound cancellation of this experiment might contain higher-dimensional interactions, not necessary a one-dimensional (1-D) phenomenon only (e.g., plane waves).

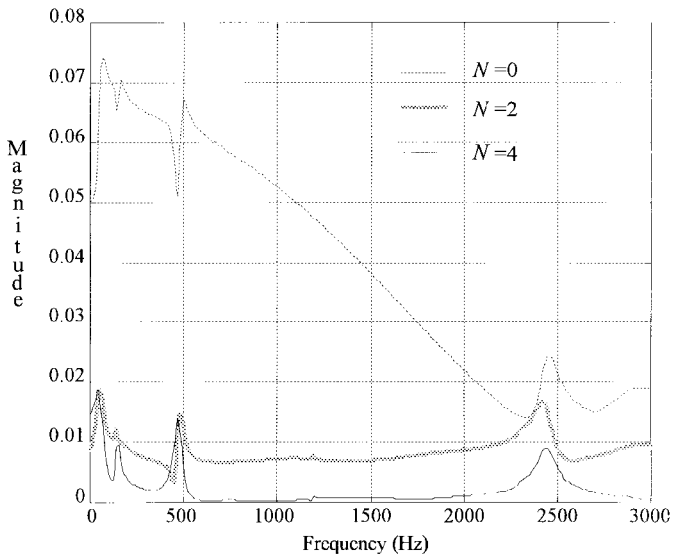


Fig. 6. Frequency response of error function $E = T_1 - T_2C$ by the $\mathbf{H}_2$ design without weighting.

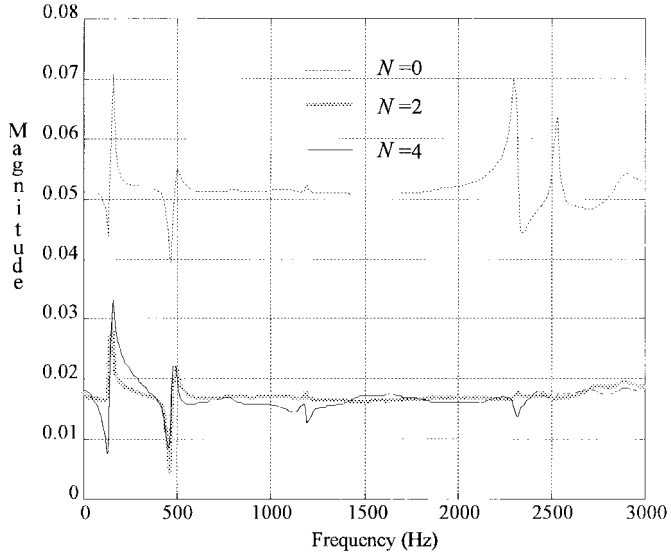


Fig. 7. Frequency response of error function $E = T_1 - T_2C$ by the $\mathbf{H}_\infty$ design without weighting.

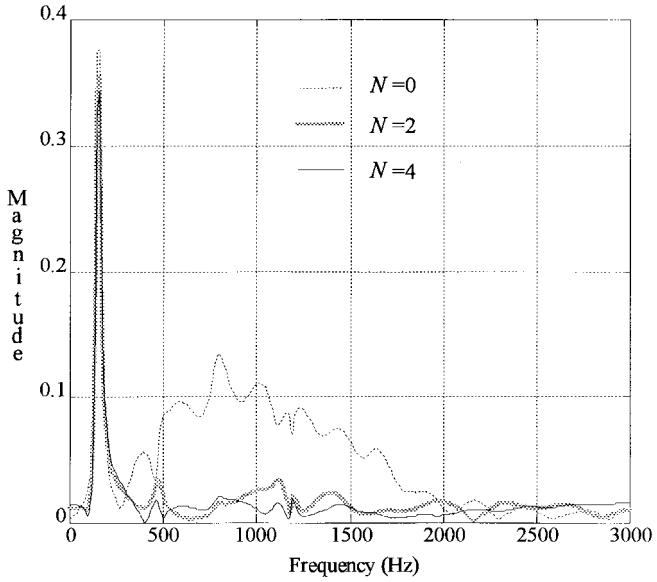


Fig. 8. Frequency response of error function $E = T_1 - T_2C$ by the $\mathbf{l}_2$ design without weighting.

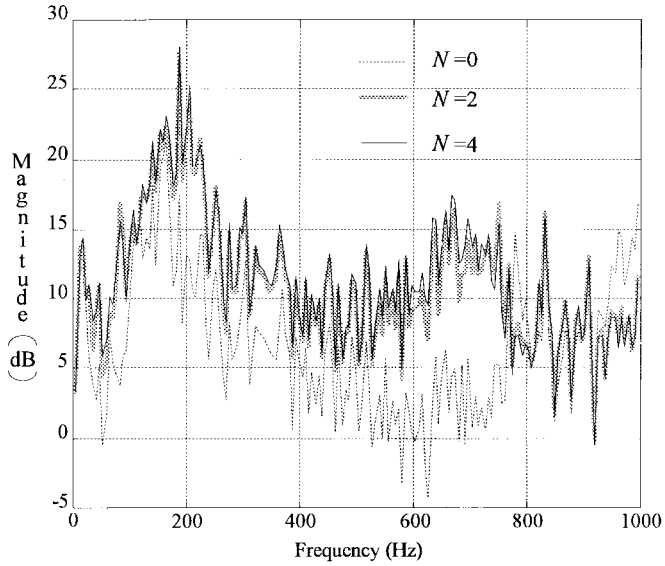


Fig. 9. Noise reduction by the $\mathbf{H}_2$-designed feedforward control without weighting.

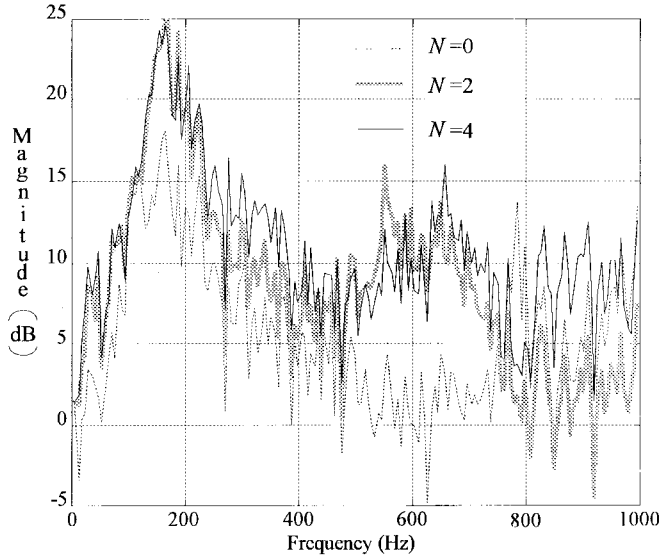


Fig. 10. Noise reduction by the $\mathbf{H}_\infty$-designed feedforward control without weighting.

Second, the plant going through speaker B ($T_1$) has a transmission zero close to the unit circle (around 700 Hz). This is usually called antiresonance and the frequency is related to the characteristic length (dimensions) of the duct.

## IV. Experimental Results

The algorithms described Section II were applied to design various feedforward controllers according to the measurement in (3). Two weighting functions were considered in the experiments: $W = 1$ (no weighting) and

$$W(z^{-1}) = 0.0037 + 0.0070z^{-1} - 0.0814z^{-2} + 0.2220z^{-3} + 0.0697z^{-4} + 0.2220z^{-5} - 0.0814z^{-6} + 0.0070z^{-7} + 0.0037z^{-8}. \quad (8)$$

The latter was a low-pass filter with cutoff frequency 1 kHz. The purpose is to emphasize the effect of cancellation for the frequency range up to 1 kHz. Other than the weighting function, preview steps 0), 2), and 4) are considered separately. The controller parameters are not shown here since the listing is quite lengthy. Interested readers can consult reference [34] for more details. For the cases without a weighting function, the corresponding error functions are plotted in Figs. 6–8 in which several interesting phenomena are observed.

(O1) The averaging nature of the $\mathbf{H}_2$ method can be seen by comparing the $N = 0$ curves in these figures. Furthermore, when causality is violated ($N = 0$), The $\mathbf{H}_2$ method seems to exhibit better high-frequency performance.

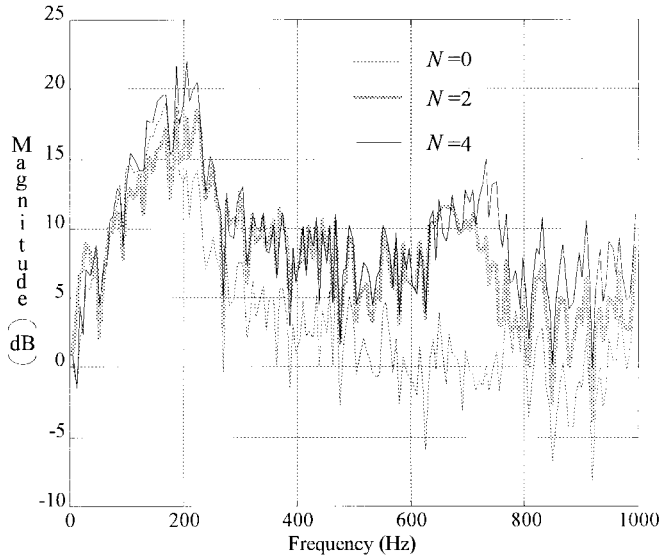


Fig. 11. Noise reduction by the $\mathbf{l}_1$-designed feedforward control without weighting.

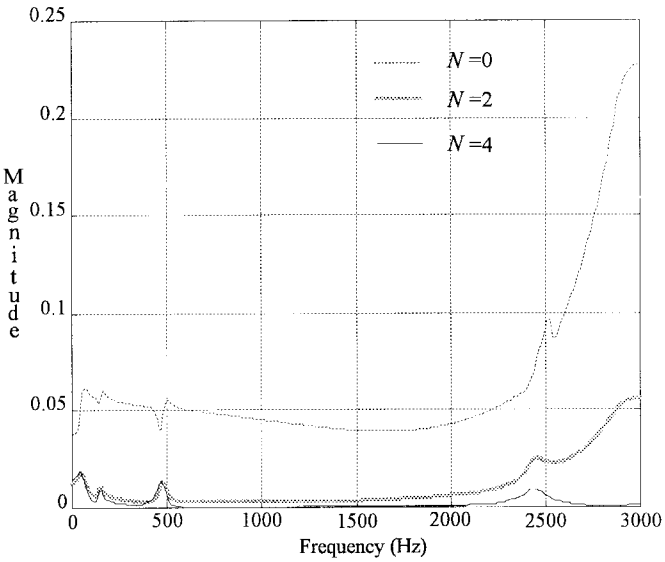


Fig. 12. Frequency response of error function $E = T_1 - T_2C$ by the $\mathbf{H}_2$ design with weighting.

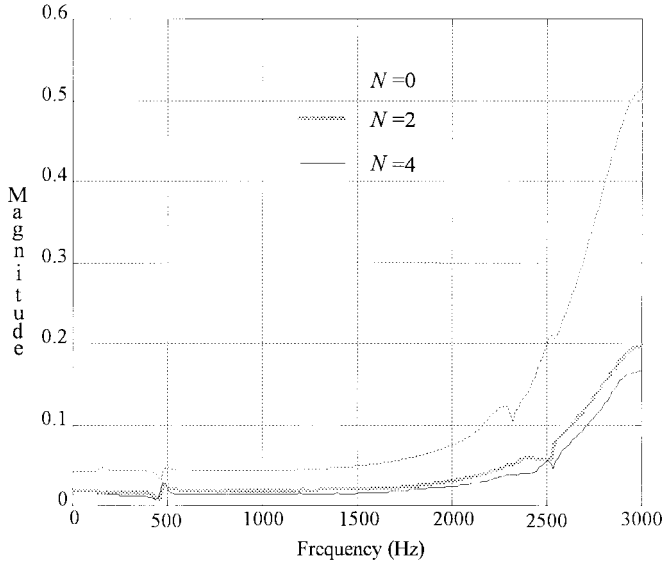


Fig. 13. Frequency response of error function $E = T_1 - T_2C$ by the $\mathbf{H}_\infty$ design with weighting.

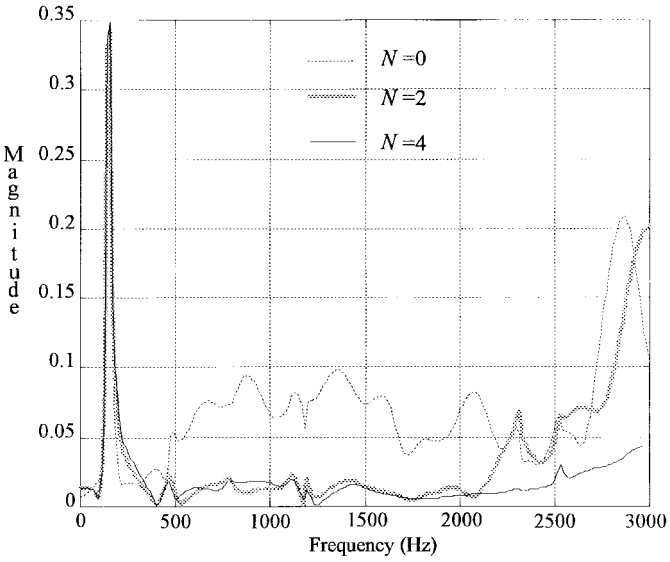


Fig. 14. Frequency response of error function $E = T_1 - T_2C$ by the $\mathbf{l}_1$ design with weighting.

(O2) The spike shown in the $\mathbf{l}_1$ design is located at the first resonance frequency of the duct system (around 187 Hz, see Fig. 5). Most interestingly, while the other two methods showed significant reduction in relative error around this frequency when preview steps were increased, the reduction by the $\mathbf{l}_1$ design was limited. However, this phenomenon is not repeated at the second resonance frequency (around 475 Hz). A careful examination of Fig. 5 reveals that the peak level of $T_1$ (noise transmission path) is greater than that of $T_2$ (control signal transmission path) at the first resonance and vice versa at the second resonance. This shows that designers must be careful in applying the $\mathbf{l}_1$ design method to flexible systems.

(O3) When $N = 4$, the control signal led the noise signal by two digital steps. However, the improvement in error was not significant compared with $N = 2$ because the noncausal part of the stable inverse of $T_2$ (i.e., its Laurent series) did not have much influence on the performance.

The steady-state noise reductions achieved by implementing these design methods are plotted in Figs. 9–11. These figures show the difference of spectrum magnitude measured by the error microphone (Fig. 4) before and after the controller is turned on. The results lead to the following observations.

(O4) Although the causality principle was violated when $N = 0$, noise level was still reduced. Without loss of generality, assume that the noise transmission path ($T_1$, see Fig. 1) has no delay and the control

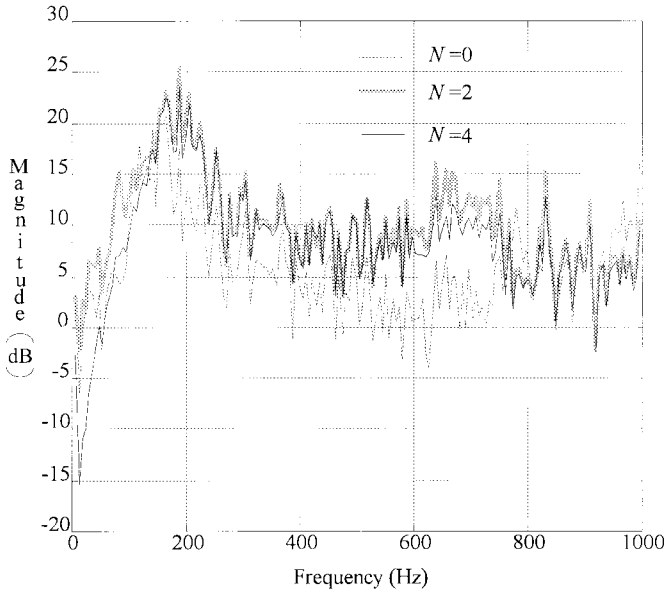


Fig. 15. Noise reduction by the $\mathbf{H}_2$-designed feedforward control with weighting.

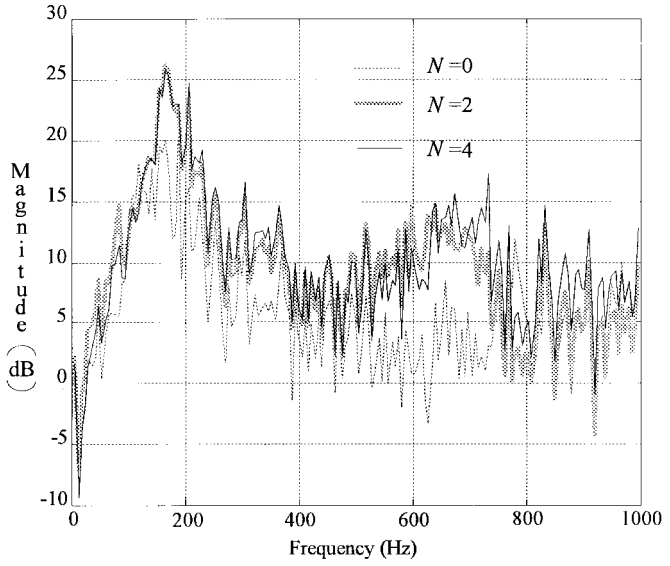


Fig. 16. Noise reduction by the $\mathbf{H}_\infty$-designed feedforward control with weighting.

sound transmission path (including the controller, $T_2C$) has $m$-step delay. Further, assume that the impulse response of $T_1$ be $\sum_{i=0}^{\infty} a_i z^{-1}$ and $T_2C$ be $\sum_{i=m}^{\infty} b_i z^{-1}$, the resulting variance of the error $e(k)$ subject to a zero-mean white noise $d(k)$ (variance $= E[d^2]$) is

$$E[e^2(k)] = \sum_{i=0}^{m-1} a_i^2 E[d^2] + \sum_{i=m}^{\infty} (a_i - b_i)^2 E[d^2].$$

Therefore, as long as the error signal produced through $T_1$ depends on the noise signal in the past (i.e., $a_i \neq 0$ for $i \geq m$ in the above equation), it is possible to reduce the variance of $e(k)$ by a proper design of $C$. Similar analysis can be conducted if we look at the magnitude of $e(k)$. Considering the noise cancellation in free space where $T_1$ is characterized by pure delay, it is easy to see that it is impossible to reduce the error variance or magnitude unless the causality principle is observed. In a confined-space problem, since noise bounces back and forth among boundaries, the dependency of current noise signal in any point and past noise source signal could be strong. Therefore, it is still possible to reduce the noise level even if the causality principle is violated.

(O5) Observation (O2.) is verified by comparing the noise reductions around 187 Hz of Figs. 9–11. The $\mathbf{l}_1$ design does have inferior performance at resonance.

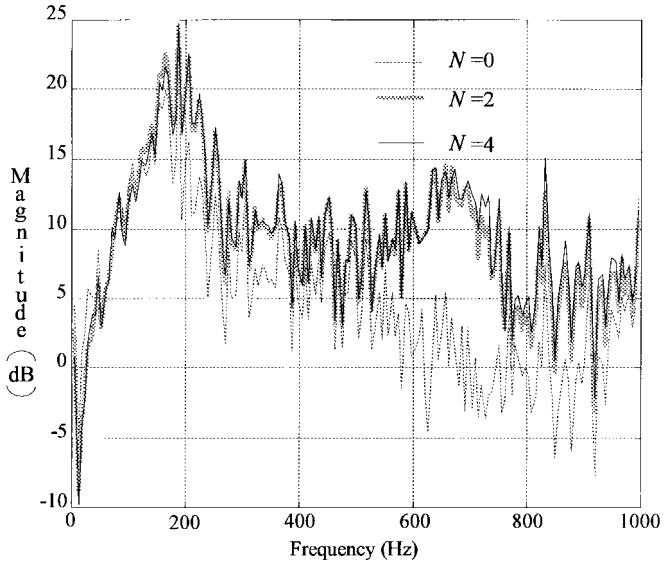


Fig. 17. Noise reduction by the $\mathbf{l}_1$-designed feedforward control with weighting.

Experimental results from the controllers designed with weighting are depicted in Figs. 12–17. Figs. 12–14 clearly show that performance in the low-frequency range is enhanced, so as the noise reduction in experiments (Figs. 15–17). Notice that the reduction levels in the range between 0–50 Hz were worse than the no-weighting cases. Although this is unimportant since sound in this range is hardly audible, the phenomenon is worth further investigation. One possibility might be that the speakers produce sound nonlinearly at very low frequencies (e.g., harmonic distortion).

The analyzes presented thus far are based on objective evaluations. However, the ultimate goal of noise reduction is human comfort. Thus, subjective evaluations are very important. While many psychoacoustic indexes are available (such as annoyance, see [26]), we use A-weighting, C-weighting and linear weighting (no weight) to measure the differences among the design methods [24]. A-weighting is intended to be such that sounds of different frequencies giving the same decibel reading with this weighting could be equally loud. As a result, less emphasis is placed around low (less than 1000 Hz) and high (greater than 6000 Hz) frequency range. C-weighting is different from A-weighting by emphasizing a larger frequency range (about 100–4000 Hz) and a smaller roll-off rate among

TABLE IV
FREQUENCY-WEIGHTED-AVERAGE REDUCTION OF NOISE (NO-WEIGHTING CASES)

| | | A-Weighting | | C-Weighting | | Linear-Weighting | |
|---|---|---|---|---|---|---|---|
| Background noise | | 44.9 dB | | 59.8 dB | | 64.9 dB | |
| Uncanceled noise | | 77.9 dB | | 89.8 dB | | 89.9 dB | |
| | $N$ | dB | Reduction | dB | Reduction | dB | Reduction |
| $\mathbf{H}_2$ | 0 | 71.8 | 6.1 | 77.7 | 12.1 | 77.9 | 12.0 |
| | 2 | 69.3 | 8.6 | 74.2 | 15.6 | 77.8 | 12.1 |
| | 4 | 69.0 | 8.9 | 73.9 | 15.9 | 77.1 | 12.8 |
| $\mathbf{H}_\infty$ | 0 | 71.8 | 6.1 | 77.6 | 12.2 | 78.1 | 11.8 |
| | 2 | 70.2 | 7.7 | 73.7 | 16.1 | 76.5 | 13.4 |
| | 4 | 68.4 | 9.5 | 72.2 | 17.6 | 73.5 | 16.4 |
| $l_1$ | 0 | 72.2 | 5.7 | 77.4 | 12.4 | 77.9 | 12.0 |
| | 2 | 69.8 | 8.1 | 75.1 | 14.7 | 77.6 | 12.3 |
| | 4 | 68.9 | 9.0 | 74.0 | 15.8 | 74.4 | 12.5 |

TABLE V
FREQUENCY-WEIGHTED-AVERAGE REDUCTION OF NOISE (WEIGHTED CASES)

| | | A-Weighting | | C-Weighting | | Linear-Weighting | |
|---|---|---|---|---|---|---|---|
| Background noise | | 45.0 dB | | 61.1 dB | | 64.4 dB | |
| Uncanceled noise | | 79.2 dB | | 91.1 dB | | 91.2 dB | |
| | $N$ | dB | Reduction | dB | Reduction | dB | Reduction |
| $\mathbf{H}_2$ | 0 | 73.3 | 5.9 | 78.8 | 12.3 | 78.9 | 12.3 |
| | 2 | 70.0 | 9.2 | 75.1 | 16.0 | 75.5 | 15.7 |
| | 4 | 69.8 | 9.4 | 75.0 | 16.1 | 75.5 | 15.7 |
| $\mathbf{H}_\infty$ | 0 | 75.9 | 3.3 | 79.4 | 11.7 | 80.0 | 11.2 |
| | 2 | 70.4 | 8.8 | 74.2 | 16.9 | 74.3 | 16.9 |
| | 4 | 70.3 | 8.9 | 73.9 | 17.2 | 74.4 | 16.8 |
| $l_1$ | 0 | 73.0 | 6.2 | 78.1 | 13.0 | 78.4 | 12.8 |
| | 2 | 70.0 | 9.2 | 75.2 | 15.9 | 75.2 | 16.0 |
| | 4 | 69.8 | 9.4 | 75.4 | 15.7 | 75.5 | 15.7 |

lower frequencies. Hence, C-weighting is usually used in a low-frequency noise environment. The measurements were taken with a B&K sound-level meter (Fig. 4) and results are recorded in Tables IV and V. These figures do not show much difference among the design methods. Moreover, adding the proposed weighting function (8) in optimization does not improve the performance. Most of the differences are less than 1 dB which is likely to be a measurement error.

## V. CONCLUSION

Model-matching techniques are useful tools for designing feedforward controllers, especially when a broad-band performance is required. This paper applies digital model-matching techniques using $\mathbf{H}_2$, $\mathbf{H}_\infty$, and $\mathbf{l}_1$ measures to design feedforward controllers for active noise cancellation in ducts. From a signal-processing standpoint, these techniques provide a systematic way of approximating the inverse of a nonminimum phase filter in stable domain. It has been shown that the performance (values of error norms) can be enhanced if future inputs are available. A simple example demonstrates that with preview action, the inverse of a nonminimum phase zero is simply given as its truncated Laurent series in the corresponding convergence domain (the anticausal part). Experimental results show significant broad-band reduction of noise. They also prove that by applying the concept of model-matching, it is not necessary to observe the causality principle in order to achieve active noise reduction.

## REFERENCES

[1] M. D. Alter and T. C. Tsao, "Control of linear motors for machine tool feed drives, Part II: Experimental investigation of optimal feedforward tracking control," in *Workshop on Advanced High-Speed/High Precision Control Technology,* Taipei, Taiwan, 1994.
[2] K. J. Astrom, P. Hagander, and J. Sternby, "Zeros of sampled systems," *Automatica,* vol. 20, no. 1, 1984.
[3] J. A. Cadzow, "Functional analysis and the optimal control of linear discrete systems," *Int. J. Contr.,* vol. 17, no. 3, pp. 481–495, 1973.
[4] M. A. Dahleh and J. B. Pearson, "$\mathbf{l}_1$-optimal feedback controllers for discrete-time systems," in *Proc. Amer. Contr. Conf.,* June 1986, pp. 1964–1968.
[5] ——, "$\mathbf{l}_1$-optimal feedback controllers for MIMO discrete-time systems," *IEEE Trans. Automat. Contr.,* vol. AC-32, pp. 314–322, Apr. 1987.
[6] J. C. Doyle, B. A. Francis, and A. R. Tannenbaum, *Feedback Control Theory.* New York: Macmillan, 1992.
[7] L. J. Eriksson, M. C. Allie, and R. A. Greiner, "The selection and application of an IIR adaptive filter for use in active sound attenuation," *IEEE Trans. Acoust., Speech, Signal Processing,* vol. ASSP-33, 1987.

[8] L. J. Eriksson, "Development of filtered-U algorithm for active noise control," *J. Acoust. Soc. Amer.*, vol. 89, pp. 257–265, 1987.
[9] B. A. Francis, "On the Wiener–Hopf approach to optimal feedback design," *Syst. Contr. Lett.*, vol. 2, pp. 197–201, 1982.
[10] ——, "A course in $\mathbf{H}_\infty$ control theory," in *Lecture Notes in Control and Information Science*, vol. 88. New York: Springer-Verlag, 1987.
[11] Y. Funahashi and M. Yamada, "Zero phase error tracking controllers with optimal gain characteristics," *ASME J. Dynamic Syst., Meas., Contr.*, vol. 115, pp. 311–318, 1993.
[12] R. T. Gorden and W. D. Vining, "Active noise control: A review of the field," *Amer. Ind. Hygiene Assoc. J.*, vol. 53, no. 11, Nov. 1992.
[13] E. Gross and M. Tomizuka, "Experimental flexible beam tip tracking control with a truncated series approximation to uncancelable inverse dynamics," *IEEE Trans. Contr. Syst. Technol.*, vol. 2, pp. 382–391, Dec. 1994.
[14] D.-W. Gu, M. C. Tsai, S. D. O'Young, and I. Postlethwaite, "State-space formulae for discrete-time $\mathbf{H}_\infty$ optimization," *Int. J. Contr.*, vol. 49, no. 5, pp. 1683–1723, 1989.
[15] M. E. Halpern, "Preview tracking for discrete-time SISO systems," *IEEE Trans. Automat. Contr.*, vol. 39, pp. 589–592, Mar. 1994.
[16] J. Hu, "Active sound cancellation of finite length duct using close-form transfer function models," *ASME J. Dynamic Syst., Meas., Contr.*, vol. 118, no. 2, pp. 372–378, 1995.
[17] K. Ichikawa, *Control System Design Based on Exact Model-Matching Techniques.* Berlin: Springer-Verlag, 1985.
[18] D. Kavranoglou *et al.*, "$\mathbf{H}_\infty$ optimal feedforward process control," in *1992 Amer. Contr. Conf.*, 1992.
[19] D. Kavranoglou and M. Bettayeb, "Direct state-space solution to the discrete-time $\mathbf{H}_\infty$ one block problem," *IEEE Trans. Automat. Contr.*, vol. 38, pp. 606–611, 1993.
[20] P. Lueg, "Process of silencing sound oscillator," U.S. Patent 2 043 416, 1936.
[21] D. G. Luenberger, *Optimization by Vector Space Methods.* New York: Wiley, 1969.
[22] C. Menq and Z. Xia, "Characterization and compensation of discrete-time nonminimum phase zeros for precision tracking control," in *Proc. 1991 Winter Annu. Meet.*, 1991.
[23] P. A. Nelson and S. J. Elliott, "Active noise control: A tutorial review," *IEICE Trans. Fundamentals*, vol. E75-A, no. 11, Nov. 1992.
[24] A. D. Pierce, *Acoustics: An Introduction to Its Physical Principles and Applications*. New York: Acoust. Soc. Amer., 1991.
[25] D. A. Pierre and P. E. Uhlrich, "Look-ahead control algorithm for computer control of machine tools," in *Proc. J. Automat. Contr. Conf.*, Charlottesville, VA, June 1981.
[26] C. G. Rice and J. G. Walker, *Subjective Acoustics, Noise and Vibration.* New York: Wiley, 1982, ch. 28.
[27] A. Roure, "Self-adaptive broadband active sound control system," *J. Sound Vibration*, vol. 101, pp. 429–441, 1985.
[28] M. Tomizuka and D. E. Whitney, "Optimal discrete finite preview problems (why and how is future information important?)," *ASME J. Dynamic Syst., Meas., Contr.*, vol. 97, pp. 319–325, Dec. 1975.
[29] M. Tomizuka and D. H. Fung, "Design of digital feedforward/preview controllers for processes with predetermined feedback controllers," *ASME J. Dynamic Syst., Meas., Contr.*, vol. 102, pp. 218–225, Dec. 1980.
[30] M. Tomizuka, "Zero-phase error tracking algorithm for digital control," *ASME J. Dynamic Syst., Meas., Contr.*, vol. 109, pp. 65–68, 1987.
[31] T. C. Tsao, "Optimal feed-forward digital tracking controller design," *ASME J. Dynamic Syst., Meas., Contr.*, vol. 116, pp. 583–592, 1994.
[32] T. Yahagi, and J. Lu, "Jianming, On self-tuning control of nonminimum phase discrete-time systems using approximate inverse systems," *ASME J. Dynamic Syst., Meas., Contr.*, vol. 115, pp. 12–18, Mar. 1993.
[33] F. B. Yeh and C. D. Yang, *Post Modern Control Theory and Design.* Taiwan: Eurasia, 1992.
[34] S.-H. Yu, "Design of active noise controllers using time and frequency domain optimization techniques," Master's thesis, Dept. Contr. Eng., National Chao Tung Univ., Hsinchu, Taiwan, R.O.C.
[35] M. Vidyasagar, "Optimal rejection of persistent bounded disturbances," *IEEE Trans. Automat. Contr.*, vol. AC-31, pp. 527–534, June 1986.
[36] B. Widrow *et al.*, "Adaptive noise cancelling: Principles and application," *Proc. IEEE*, vol. 63, pp. 1692–1716, Dec. 1975.

**Jwu-Sheng Hu** received the B.S. degree from the Department of Mechanical Engineering, National Taiwan University, Taiwan, in 1984, and the M.S. and Ph.D. degrees from the Department of Mechanical Engineering, University of California at Berkeley, in 1988 and 1990, respectively.

He is currently an Associate Professor in the Department of Control Engineering, National Chiao-Tung University, Taiwan. His current research interests include active noise control, real-time system design, and applications of digital signal processors.

**Shiang-Hwua Yu** received the B.S. degree from the Department of Mechanical Engineering, National Chung-Hsing University, Taiwan, in 1993, and the M.S. degree from the Department of Control Engineering, National Chiao-Tung University, Taiwan, in 1995.

He is now serving in the Chinese Army.

**Cheng-Shiang Hsieh** received the B.S. degree from the Department of Electrical Engineering, National Cheng-Kung University, Taiwan, in 1989, and the M.S. degree from the Department of Control Engineering, National Chiao-Tung University, Taiwan, in 1995.

He is now working at Taiwan Semiconductor Manufacturing Co. (TSMC) as an Equipment Engineer.